Cosmological Studies with Gamma-Ray Bursts

Abraham Loeb

Astronomy Department, Harvard University
Cambridge, MA 02138, USA

Abstract. Gamma-Ray Burst (GRB) explosions from the first generation of stars offer an exciting opportunity to probe the epoch of reionization. Clues about how and when the intergalactic medium was ionized can be read off their UV emission spectrum. Roughly a percent of all GRBs should be strongly gravitationally lensed by intervening stars. A microlensed lightcurve can be inverted to reconstruct the surface brightness profile of the GRB image on the sky, with micro–arcsecond resolution.

1 Introduction

Since their discovery four decades ago, quasars have been used as powerful lighthouses which probe the intervening universe out to high redshifts, $z \sim 6$ ([25,9]). The spectra of almost all quasars show strong emission lines of metals, indicating super-solar enrichment of the emitting gas [24]. This implies that at least in the cores of galaxies, formation of massive stars and their evolution to supernovae preceded the observed quasar activity. If Gamma-Ray Bursts (GRBs) originate from the remnants of massive stars (such as neutron stars or black holes), as seems likely based on recent estimates of their energy output [45,11,10], then they should exist at least out to the same redshift as quasars. Although GRBs are transient events, their peak optical-UV flux can be as bright as that of quasars. Hence, GRBs promise to be as useful as quasars in probing the high–redshift universe.

Not much is known observationally about the universe in the redshift interval $z = 6$–30, when the first generation of galaxies condensed out of the primordial gas left over from the Big Bang (see reviews [3] and [30]). Observations of the microwave background anisotropies indicate that the cosmic gas became neutral at $z \sim 1000$ and remained so at least down to $z \sim 30$ (see, e.g. [43]). On the other hand, the existence of transmitted flux shortward of the Lyα resonance in the spectrum of the highest-redshift quasars and galaxies (see, for example, Figure 1), indicates that the intergalactic medium was reionized to a level better than 99.9999% by a redshift $z \sim 6$. This follows from the fact that the Lyα optical depth of the intergalactic medium at high-redshifts ($z \gg 1$) is [22],

$$\tau_\alpha = \frac{\pi e^2 f_\alpha \lambda_\alpha n_{HI}(z)}{m_e c H(z)} \approx 6.45 \times 10^5 x_{HI} \left(\frac{\Omega_b h}{0.03}\right) \left(\frac{\Omega_m}{0.3}\right)^{-1/2} \left(\frac{1+z}{10}\right)^{3/2}, \quad (1)$$

where $H \approx 100h$ km s^{-1} Mpc$^{-1}\Omega_m^{1/2}(1+z)^{3/2}$ is the Hubble parameter at the source redshift z, $f_\alpha = 0.4162$ and $\lambda_\alpha = 1216$Å are the oscillator strength and

the wavelength of the Lyα transition; $n_{HI}(z)$ is the average intergalactic density of neutral hydrogen at the source redshift (assuming primordial abundances); Ω_m and Ω_b are the present-day density parameters of all matter and of baryons, respectively; and x_{HI} is the average fraction of neutral hydrogen. Modeling [9] of the transmitted flux in Figure 1 implies $\tau_\alpha < 0.5$ or $x_{HI} < 10^{-6}$, i.e., the low-density gas throughout the universe is fully ionized at $z \sim 6$!

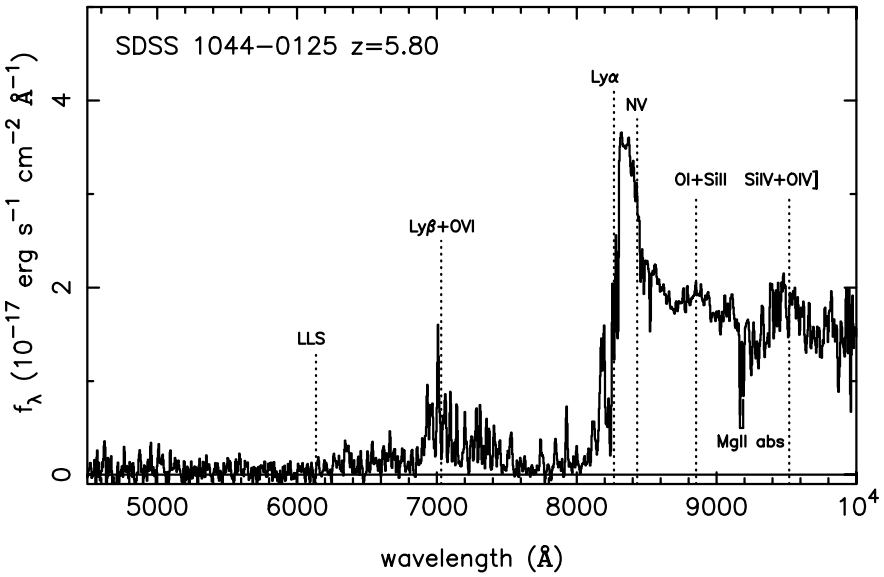

Fig. 1. Optical spectrum of a $z = 5.8$ quasar, discovered by the Sloan Digital Sky Survey (Fan et al. 2000).

The question: *how and when was the universe reionized?* defines a new frontier in observational cosmology [30]. The UV spectrum of GRB afterglows can be used to probe the ionization and thermal state of the intergalactic gas during the epoch of reionization, at redshifts $z \sim 7$–10 [33]. The stretching of the temporal evolution of GRB lightcurves by the cosmological redshift factor $(1 + z)$, makes it easier for an observer to react in time and take a spectrum of their optical-UV emission at its peak.

Energy arguments suggest that reionization resulted from photoionization rather than from collisional ionization [42,14]. The corresponding sources of UV photons were either stars or quasars. Recent simulations of the first generation of stars that formed out of the primordial metal–free gas indicate that these stars were likely massive [6,1]. If GRBs result from compact stellar remnants, such as black holes or neutron stars, then the fraction of all stars that lead to GRBs may have been higher at early cosmic times. This, however, is true only if the GRB phenomena is triggered on a time scale much shorter than the age of the universe at the corresponding redshift, which for $z \gg 1$ is $\sim$

5.4×10^8 yr $(h/0.7)^{-1}(\Omega_m/0.3)^{-1/2}[(1+z)/10]^{-3/2}$. This condition may not hold, for example, for neutron star binaries with an excessively long coalescence time.

In §2 we briefly discuss the expected properties of GRB afterglows at high redshift. We then describe the use of distant GRBs for two studies: (i) probing the intergalactic medium (IGM) during the epoch of reionization (§3); and (ii) finding intervening stars at cosmological distances through their gravitational lensing effect (§4).

2 Properties of High-Redshift GRB Afterglows

Young (days to weeks old) GRBs outshine their host galaxies in the optical regime. In the standard hierarchical model of galaxy formation, the characteristic mass and hence optical luminosity of galaxies and quasars declines with increasing redshift [23,41,3]. Hence, GRBs should become easier to observe than galaxies or quasars at increasing redshift. Similarly to quasars, GRB afterglows possess broad-band spectra which extend into the rest-frame UV and can probe the ionization state and metallicity of the IGM out to the epoch when it was reionized at a redshift $z \sim 7$–10 [30]. Lamb & Reichart [29] have extrapolated the observed γ-ray and afterglow spectra of known GRBs to high redshifts and emphasized the important role that their detection might play in probing the IGM. Simple scaling of the long-wavelength spectra and temporal evolution of afterglows with redshift implies that at a fixed time lag after the GRB trigger in the observer's frame, there is only a mild change in the *observed* flux at infrared or radio wavelengths as the GRB redshift increases. Ciardi & Loeb [7] demonstrated this behaviour using a detailed extrapolation of the GRB fireball solution into the non-relativistic regime (see the 2μm curves in Figure 2). Despite the strong increase of the luminosity distance with redshift, the observed flux for a given observed age is almost independent of redshift in part because of the special spectrum of GRB afterglows (see Figure 4), but mainly because afterglows are brighter at earlier times and a given observed time refers to an earlier intrinsic time in the source frame as the source redshift increases. The mild dependence of the long-wavelength ($\lambda_{\rm obs} > 1\mu$m) flux on redshift differes from other high-redshift sources such as galaxies or quasars, which fade rapidly with increasing redshift [23,41,3]. Hence, GRBs provide exceptional lighthouses for probing the universe at $z = 6$–30, at the epoch when the first stars had formed.

Assuming that the GRB rate is proportional to the star formation rate and that the characteristic energy output of GRBs is $\sim 10^{52}$ ergs, Ciardi & Loeb [7] predicted that there are always ~ 15 GRBs from redshifts $z > 5$ across the sky which are brighter than ~ 100 nJy at an observed wavelength of $\sim 2\mu$m. The infrared spectrum of these sources could be taken with future telescopes such as the *Next Generation Space Telescope* (planned for launch in 2009; see http://ngst.gsfc.nasa.gov/), as a follow-up on their early X-ray localization with the *Swift* satellite (planned for launch in 2003; see http://swift.sonoma.edu/).

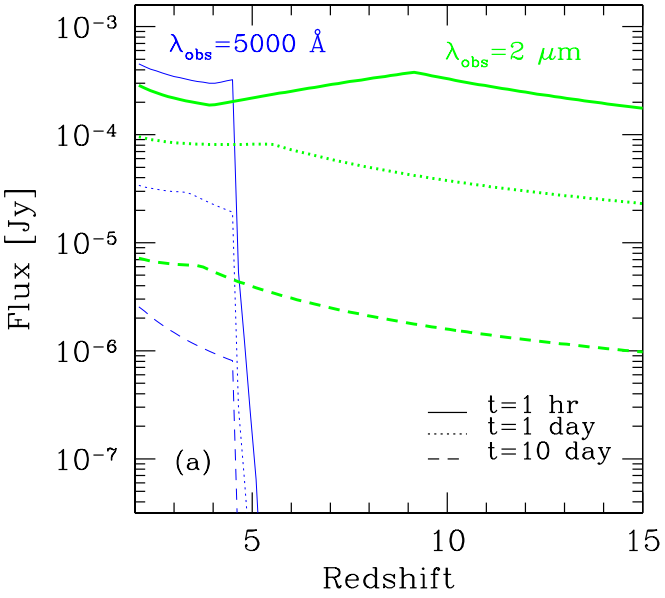

Fig. 2. Theoretical expectation for the observed afterglow flux of a GRB as a function of its redshift (from Ciardi & Loeb 2000). The curves refer to an observed wavelength of 5000 Å(thin lines) and 2μm (thick lines). Different line types refer to different observed times after the GRB trigger, namely 1 hour (solid line), 1 day (dotted) and 10 days (dashed). The 5000Å flux is strongly absorbed at $z > 4.5$ by intergalactic hydrogen. However, at infrared and radio wavelengths the observed afterglow flux shows only a mild dependence on the source redshift.

The redshifts of GRB afterglows can be estimated photometrically from either the Lyman limit or Lyα troughs in their spectra. At low redshifts, the question of whether the Lyman limit or Lyα trough interpretation applies depends on the absorption properties of the host galaxy. If the GRB originates from within the disk of a star–forming galaxy, then the afterglow spectrum will likely show a damped Lyα trough. At $z > 6$ the Lyα trough would inevitably exist since the intergalactic Lyα opacity is $> 90\%$ (see Figure 13 in [41]). Interestingly, an absorption feature in the afterglow spectrum which is due to the neutral hydrogen within a molecular cloud or the disk of the host galaxy, is likely to be time-dependent due to the ionization caused by the UV illumination of the afterglow itself along the line-of-sight [37].

So far, there have been two claims for high-redshift GRBs. Fruchter [12] argued that the photometry of GRB 980329 is consistent with a Lyα trough due to IGM absorption at $z \sim 5$. Anderson et al. [2] inferred a redshift of $z = 4.5$ for GRB 000131 based on a crude optical spectrum that was taken by the VLT a few days after the GRB trigger. *These cases emphasize the need for a coordinated observing program that will alert 10-meter class telescopes to*

take a spectrum of an afterglow about a day after the GRB trigger, based on a photometric assessment (obtained with a smaller telecope using the Lyman limit or Lyα troughs) that the GRB may originate at a high redshift.

In the following two sections, we use two examples to illustrate the usefulness of GRB afterglows for cosmological studies.

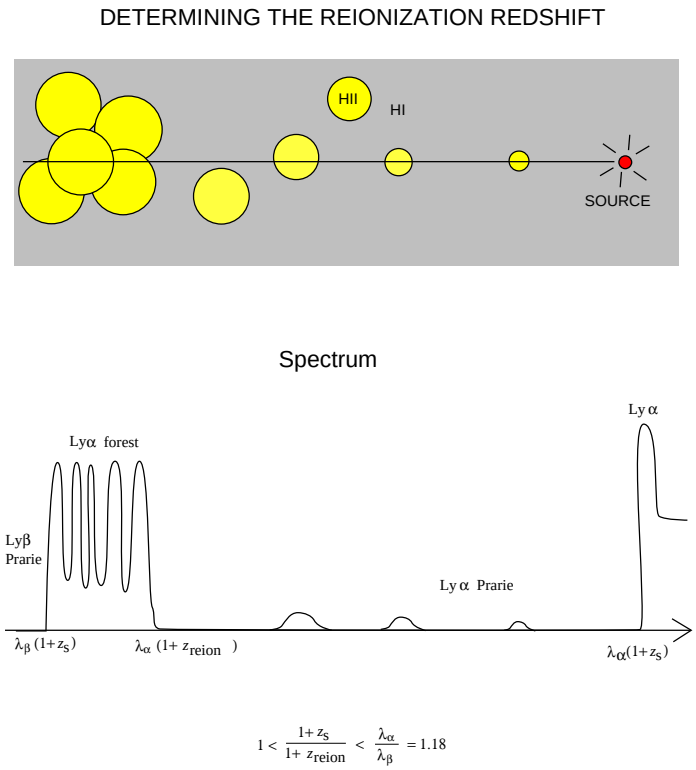

Fig. 3. Sketch of the expected spectrum of a source at a redshift z_s slightly above the reionization redshift $z_{\rm reion}$. The transmitted flux due to HII bubbles in the pre-reionization era, and the Lyα forest in the post-reionization era, are exaggerated for illustration.

3 Probing the Intergalactic Medium

The UV spectra of GRB afterglows can be used to measure the evolution of the neutral intergalactic hydrogen with redshift. Figure 3 illustrates schematically the expected absorption just beyond the reionization redshift. Resonant scattering suppresses the spectrum at all wavelengths corresponding to the Lyα resonance prior to reionization. Since the Lyα cross-section is very large, any

transmitted flux prior to reionization reflects a large volume of ionized hydrogen along the line-of-sight. If the GRB is located at a redshift larger by $> 18\%$ than the reionization redshift, then the Lyα and the Lyβ troughs will overlap. Unlike quasars, GRBs do not ionize the IGM around them; their limited energy supply $\sim 10^{52}$ ergs [45,11,10] can ionize only $\sim 4 \times 10^5 M_\odot$ of neutral hydrogen within their host galaxy.

Quasar spectra indicate the existence of an IGM metallicity which is a fraction of a percent of the solar value [8]. The metals were likely dispersed into the IGM through outflows from galaxies, driven by either supernova or quasar winds [3,14]. Detection of metal absorption lines in the spectrum of GRB afterglows, produced either in the IGM or the host galaxy of the GRB, can help unravel the evolution of the IGM metallicity with redshift and its link to the evolution of galaxies.

4 Cosmological Microlensing of Gamma-Ray Bursts

Loeb & Perna [31] noted the coincidence between the angular size of a solar-mass lens at a cosmological distance and the micro-arcsecond size of the image of a GRB afterglow. They therefore suggested that microlensing by stars can be used to resolve the photospheres of GRB fireballs at cosmological distances. (Alternative methods, such as radio scintillations, only provide a constraint on the radio afterglow image size [18,45] but do not reveal its detailed surface brightness distribution, because of uncertainties in the scattering properties of the Galactic interstellar medium.)

The fireball of a GRB afterglow is predicted to appear on the sky as a ring (in the optical band) or a disk (at low radio frequencies) which expands laterally at a superluminal speed, $\sim \Gamma c$, where $\Gamma \gg 1$ is the Lorentz factor of the relativistic blast wave which emits the afterglow radiation [44,39,36,20]. For a spherical explosion into a constant density medium (such as the interstellar medium), the physical radius of the afterglow image is of order the fireball radius over Γ, or more precisely [20]

$$R_{\rm s} = 3.9 \times 10^{16} \left(\frac{E_{52}}{n_1}\right)^{1/8} \left(\frac{t_{\rm days}}{1+z}\right)^{5/8} \ {\rm cm}, \qquad (2)$$

where E_{52} is the hydrodynamic energy output of the GRB explosion in units of 10^{52} ergs, n_1 is the ambient medium density in units of 1 cm^{-3}, and $t_{\rm days}$ is the observed time in days. At a cosmological redshift z, this radius of the GRB image occupies an angle $\theta_{\rm s} = R_{\rm s}/D_A$, where $D_A(z)$ is the angular diameter distance at the GRB redshift, z. For the typical cosmological distance, $D_A \sim 10^{28}$ cm, the angular size is of order a micro-arcsecond (μas). Coincidentally, this image size is comparable to the Einstein angle of a solar mass lens at a cosmological distance,

$$\theta_{\rm E} = \left(\frac{4GM_{\rm lens}}{c^2 D}\right)^{1/2} = 1.6 \left(\frac{M_{\rm lens}}{1M_\odot}\right)^{1/2} \left(\frac{D}{10^{28}\ {\rm cm}}\right)^{-1/2} \ \mu{\rm as}, \qquad (3)$$

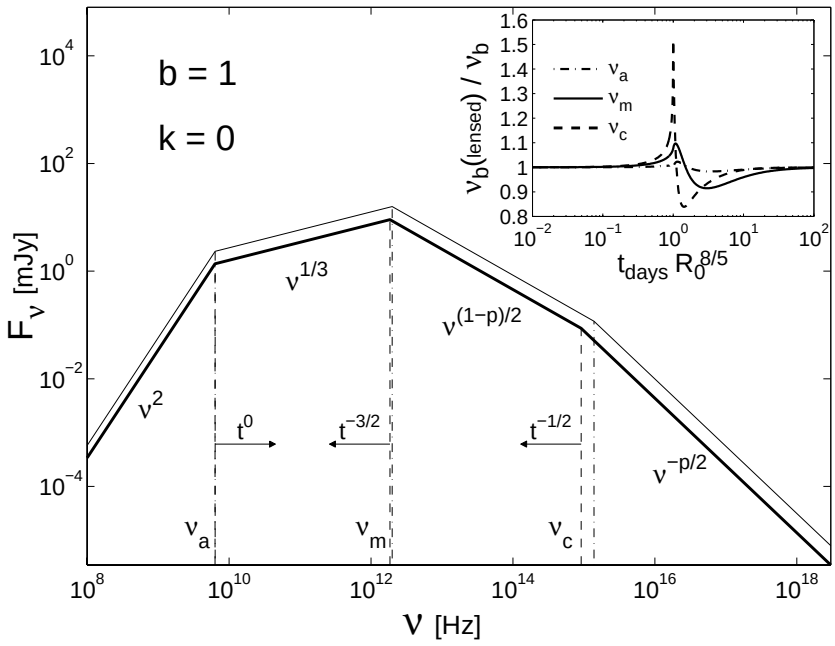

Fig. 4. A typical broken power-law spectrum of a GRB afterglow at a redshift $z = 1$ (from Granot & Loeb 2001). The observed flux density, F_ν, as a function of frequency, ν, is shown by the boldface solid line at an observed time $t_{\rm days} = 1$ for an explosion with a total energy output of 10^{52} ergs in a uniform interstellar medium ($k = 0$) with a hydrogen density of 1 cm^{-3}, and post-shock energy fractions in accelerated electrons and magnetic field of $\epsilon_e = 0.1$ and $\epsilon_B = 0.03$, respectively. The thin solid line shows the same spectrum when it is microlensed by an intervening star with an impact parameter equal to the Einstein angle and $R_0 \equiv [\theta_s(1\ {\rm day})/\theta_{\rm E}] = 1$. The insert shows the excess evolution of the break frequencies $\nu_{\rm b} = \nu_a$, ν_m and ν_c (normalized by their unlensed values) due to microlensing.

where $M_{\rm lens}$ is the lens mass, and $D \equiv D_{\rm os}D_{\rm ol}/D_{\rm ls}$ is the ratio of the angular-diameter distances between the observer and the source, the observer and the lens, and the lens and the source [40]. Loeb & Perna (1998) showed that because the ring expands laterally faster than the speed of light, the duration of the microlensing event is only a few days rather than tens of years, as is the case for more typical astrophysical sources which move at a few hundred km s^{-1} or $\sim 10^{-3}c$.

The microlensing lightcurve goes through three phases: (i) constant magnification at early times, when the source is much smaller than the source-lens angular separation; (ii) peak magnification when the ring-like image of the GRB first intersects the lens center on the sky; and (iii) fading magnification as the source expands to larger radii.

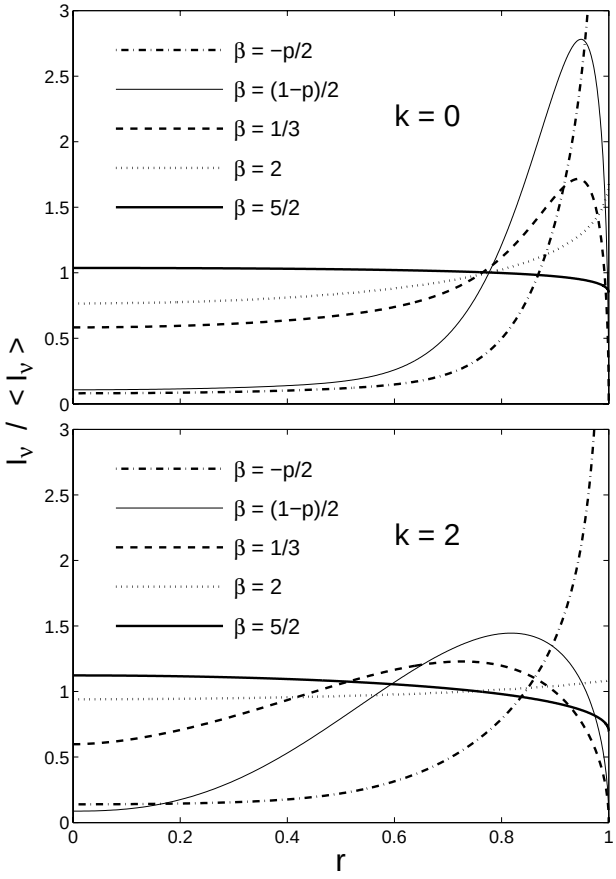

Fig. 5. The surface brightness, normalized by its average value, as a function of the normalized radius, r, from the center of a GRB afterglow image (where $r = 0$ at the center and $r = 1$ at the outer edge). The image profile changes considerably between different power-law segments of the afterglow spectrum, $F_\nu \propto \nu^\beta$ (see Figure 4). There is also a strong dependence on the power–law index of the radial density profile of the external medium around the source, $\rho \propto R^{-k}$ (taken from Granot & Loeb 2001).

Granot & Loeb [19] calculated the radial surface brightness profile (SBP) of the image of a Gamma-Ray-Burst (GRB) afterglow as a function of frequency and ambient medium properties, and inferred the corresponding magnification lightcurves due to microlensing by an intervening star. The afterglow spectrum consists of several power-law segments separated by breaks, as illustrated by Figure 4. The image profile changes considerably across each of the spectral breaks, as shown in Figure 5. It also depends on the power–law index, k, of the radial density profile of the ambient medium into which the GRB fireball propagates. Gaudi & Loeb [16] have shown that intensive monitoring of a microlensed af-

terglow lightcurve can be used to reconstruct the parameters of the fireball and its environment. The dependence of the afterglow image on frequency offers a fingerprint that can be used to identify a microlensing event and distinguish it from alternative interpretations. It can also be used to constrain the relativistic dynamics of the fireball and the properties of its gaseous environment. At the highest frequencies, the divergence of the surface brightness near the edge of the afterglow image ($r = 1$ in Figure 5) depends on the thickness of the emitting layer behind the relativistic shock front, which is affected by the length scale required for particle acceleration and magnetic field amplification behind the shock[32,21].

Ioka & Nakamura [26] considered the more complicated case where the explosion is collimated and centered around the viewing axis. More general orientations that violate circular symmetry need to be considered in the future.

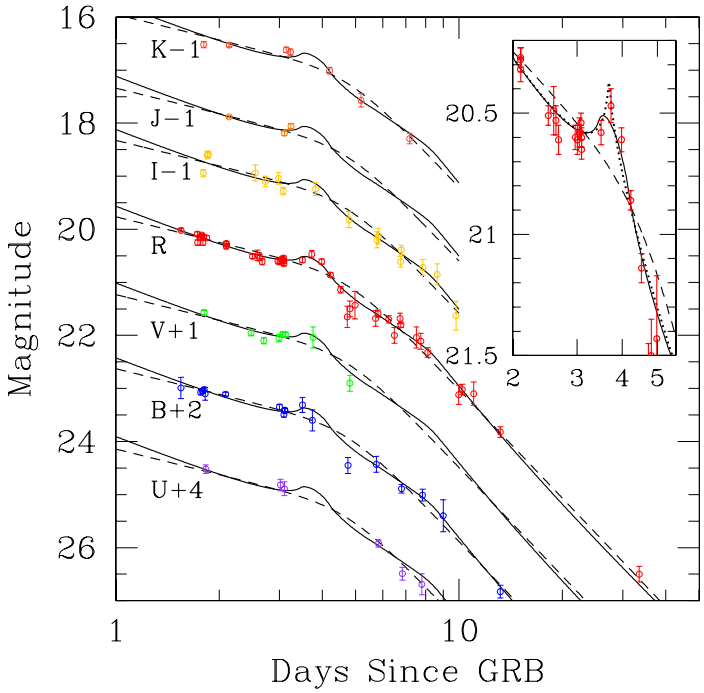

Fig. 6. *UBVRIJK* photometry of GRB 000301C as a function of time in days from the GRB trigger (from Garnavich et al. 2000; Gaudi et al. 2001). Data points have been offset by the indicated amount for clarity. The dashed line is the best-fit smooth, double power-law lightcurve (with no lensing), while the solid line is the overall best-fit microlensing model, where the SBP has been determined from direct inversion. The inset shows the *R*-band data only. The dotted line is the best-fit microlensing model with theoretically calculated SBP, for $k = 0$ and $\nu > \nu_c$.

4.1 GRB 000301C

Garnavich, Loeb, & Stanek [15] have reported the possible detection of a microlensing magnification feature in the optical-infrared light curve of GRB 000301C (see Figure 6). The achromatic transient feature is well fitted by a microlensing event of a $0.5M_{\odot}$ lens separated by an Einstein angle from the source center, and resembles the prediction of Loeb & Perna [31] for a ring-like source image with a narrow fractional width ($\sim 10\%$). Alternative interpretations relate the transient achromatic brightening to a higher density clump into which the fireball propagates [4], or to a refreshment of the decelerating shock either by a shell which catches up with it from behind or by continuous energy injection from the source [46]. However, the microlensing model has a smaller number of free parameters. If with better data, a future event will show the generic temporal and spectral characteristics of a microlensing event, then these alternative interpretations will be much less viable. A galaxy $2''$ from GRB 000301C might be the host of the stellar lens, but current data provides only an upper-limit on its surface brightness at the GRB position. The existence of an intervening galaxy increases the probability for microlensing over that of a random line-of-sight.

Gaudi, Granot, & Loeb [17] have shown that direct inversion of the observed light curve for GRB 000301C yields a surface brightness profile (SBP) of the afterglow image which is strongly limb-brightened, as expected theoretically (see Figure 7).

Obviously, realistic lens systems could be more complicated due to the external shear of the host galaxy or a binary companion. Mao & Loeb [28] calculated the magnification light curves in these cases, and found that binary lenses may produce multiple peaks of magnification. They also demonstrated that *all* afterglows are likely to show variability at the level of a few percent about a year following the explosion, due to stars which are separated by tens of Einstein angles from the line-of-sight.

What is the probability for microlensing? If the lenses are not strongly clustered so that their cross-sections overlap on the sky, then the probability for having an intervening lens star at a projected angular separation θ from a source at a redshift $z \sim 2$ is $\sim 0.3\Omega_{\star}(\theta/\theta_E)^2$ [38,5,34,35], where $\Omega_{\star}$ is the cosmological density parameter of stars. The value of $\Omega_{\star}$ is bounded between the density of the luminous stars in galaxies and the total baryonic density as inferred from Big Bang nucleosynthesis, $7 \times 10^{-3} < \Omega_{\star} < 5 \times 10^{-2}$ [13]. Hence, *all* GRB afterglows should show evidence for events with $\theta < 30\theta_E$, for which microlensing provides a small perturbation to the light curve[28]. (This crude estimate ignores the need to subtract those stars which are embedded in the dense central regions of galaxies, where macrolensing dominates and the microlensing optical depth is of order unity.) However, only one out of roughly a hundred afterglows is expected to be strongly microlensed with an impact parameter smaller than the Einstein angle. Indeed, Koopmans & Wambsganss [27] have found that the 'a posteriori' probability for the observed microlensing event of GRB 000301C along a random line-of-sight is between 0.7–2.7% if 20-100% of the dark matter is in compact objects.

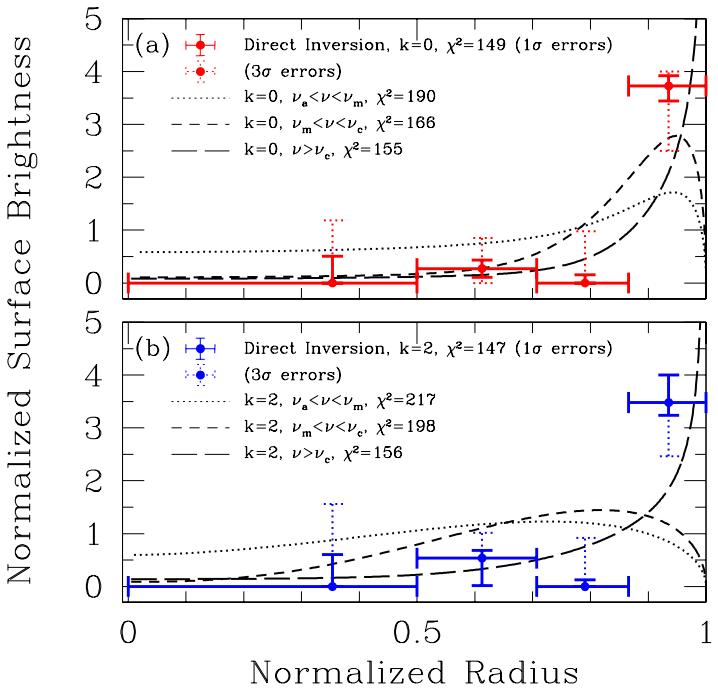

Fig. 7. Fitting GRB 000301C with different SBPs as a function of normalized radius (taken from Gaudi et al. 2001). The points are the SBPs determined from direct inversion, with 1σ errors (solid) and 3σ errors (dotted). The curves are theoretically calculated SBPs for various frequency regimes (see Figure 5). (a) Uniform external medium, $k = 0$. (b) Stellar wind environment, $k = 2$. The number of degrees of freedom is 92 for the direct inversion points and 89 for the curves.

Microlensing events are rare but precious. Detailed monitoring of a few strong microlensing events among the hundreds of afterglows detected per year by the forthcoming Swift satellite, could be used to constrain the environment and the dynamics of relativistic GRB fireballs, as well as their magnetic structure and particle acceleration process.

Acknowledgements
I thank all my collaborators on this subject: the young theorists with whom I studied the above topics – Rennan Barkana, Benedetta Ciardi, Scott Gaudi, Jonathan Granot, Zoltan Haiman, Shude Mao, Misha Medvedev, and Rosalba Perna; and the observers – Peter Garnavitch and Kris Stanek, who introduced me to the data on GRB 000301C.

References

1. T. Abel, G. Bryan, M. L. Norman: Ap. J., **540**, 39 (2000)
2. A. I. Anderson, et al.: A. & A., **364**, L54 (2000)
3. R. Barkana, A. Loeb: Physics Reports, **349**, 125 (2001)
4. E. Berger, et al.: Ap. J., **545**, 56 (2000)
5. O. M. Blaes, R. L. Webster: Ap. J., **391**, L63 (1992)
6. V. Bromm, P. S. Coppi, R. B. Larson: **527**, 5 (1999)
7. B. Ciardi, A. Loeb: Ap. J., **540**, 687 (2000)
8. S. L. Ellison, A. Songaila, J. Schaye, M. Pettini: A. J., **120**, 1175 (2000)
9. X. Fan, et al.: A. J., **120**, 1167 (2000)
10. D. A. Frail, et al.: Nature, **submitted** (2001); astro-ph/0102282
11. D. L. Freedman, E. Waxman: Ap. J., **547**, 922 (2001)
12. A. Fruchter: Ap. J., **512**, L1 (1999)
13. M. Fukugita, C. J. Hogan, P. J. E. Peebles: Nature, **366**, 309 (1998)
14. S. R. Furlanetto, A. Loeb: Ap. J., **in press**, (2001); astro-ph/0102076
15. P. M. Garnavich, A. Loeb, K. Z. Stanek: Ap. J., **544**, L11 (2000)
16. B. S. Gaudi, A. Loeb: Ap. J., **558** (2001)
17. B. S. Gaudi, J. Granot, A. Loeb: Ap. J., **in press** (2001)
18. J. Goodman: New Astronomy, **2**, 449 (1997)
19. J. Granot, A. Loeb: Ap. J., **551**, L63 (2001)
20. J. Granot, T. Piran, R. Sari: Ap. J., **513**, 679 (1999a); **527**, 236 (1999b)
21. A. Gruzinov, E. Waxman: Ap. J., **511**, 852 (1999)
22. J. E. Gunn, B. A. Peterson: Ap. J., **142**, 1633, (1965)
23. Z. Haiman, A. Loeb: Ap. J., **483**, 21 (1997); **503**, 505 (1998); **552**, 459 (2001)
24. F. Hamann, G. Ferland: A. R. A. & A. **37**, 487 (1999)
25. F. D. A. Hartwick, D. Schade: A. R. A. & A., **28**, 437 (1990)
26. K. Ioka, K., T. Nakamura: Ap. J., **in press** (2001); astro-ph/0102028
27. L. V. E. Koopmans, J. Wambsganss: M.N.R.A.S., **in press** (2001); astro-ph/0011029
28. S. Mao, A. Loeb: Ap. J., **547**, L97 (2001)
29. D. Q. Lamb, D. E. Reichart: Ap. J. **536**, 1 (2000)
30. A. Loeb, R. Barkana: ARA&A, **in press** (2001)
31. A. Loeb, R. Perna: Ap. J., **495**, 597 (1998)
32. M. V. Medvedev, A. Loeb: Ap. J. **526**, 697 (1999)
33. J. Miralda-Escudé: Ap. J., **501**, 15 (1998)
34. R. Nemiroff: Ap.& SS, **259**, 309 (1998)
35. R. Nemiroff, J. P. Norris, J. T. Bonnell, G. F. Marani: Ap. J., **494**, L173 (1998)
36. A. Panaitescu, P. Mészáros: Ap. J., **493**, L31 (1998)
37. R. Perna, A. Loeb: Ap. J., **501**, 467 (1998)
38. W. H. Press, J. E. Gunn: Ap. J., **185**, 397 (1973)
39. R. Sari: Ap. J., **494**, L49 (1998)
40. P. Schneider, J. Ehlers, E. E. Falco: *Gravitational Lenses* (Springer, Heidelberg 1992)
41. D. Stern, H. Spinrad: P. A. S. P., **111**, 1475 (1999)
42. M. Tegmark, J. Silk, A. Evrard: Ap. J., **417**, 54 (1993)
43. X. Wang, M. Tegmark, M. Zaldarriaga: **submitted** (2001); astro-ph/0105091
44. E. Waxman: Ap. J., **491**, L19 (1997)
45. E. Waxman, S. R. Kulkrani, D. A. Frail: Ap. J., **497**, 288 (1998)
46. Z. Zhang, P. Meszaros: Ap. J., **552**, L35 (2001)